

EQUILBRIUM MODELING OF TRACE METAL TRANSPORT FROM DULUTH COMPLEX ROCKPILE¹

by

Paula D. Kelsey², Ronald W. Klusman² and Kim Lapakko³

Abstract: Geochemical modeling was used to predict weathering processes and the formation of trace metal-adsorbing secondary phases in a waste rock stockpile containing Cu-Ni ore mined from the Duluth Complex, MN. Amorphous ferric hydroxide was identified as a secondary phase within the pile, from observation and geochemical modeling of the weathering process. Due to the high content of cobalt, copper, nickel, and zinc in the primary minerals of the waste rock and in the effluent, it was hypothesized that the predicted and observed precipitant ferric hydroxide would adsorb small quantities of these trace metals. This was verified using sequential extractions and simulated using adsorption geochemical modeling. It was concluded that the trace metals were adsorbed in small quantities, and adsorption onto the amorphous ferric hydroxide was in decreasing order of Cu > Ni > Zn > Co. The low degree of adsorption was due to low pH water and competition for adsorption sites with other ions in solution.

Additional Key Words: geochemical modeling, sequential extractions.

Introduction

The Duluth Complex

The Duluth Complex is a layered igneous intrusion in northeastern Minnesota which is well known as a potential future source of copper and nickel ore (Johnson, 1970 and Sims, 1967). It also contains substantial amounts of Co and platinum-group metals (Boucher, 1975). In the early 1970's AMAX Exploration Inc. began evaluating the potential of an area in the vicinity of the town of Babbitt, MN for the mining and extraction of copper and nickel (Lapakko, 1994). In 1977, a joint effort between the State of Minnesota and AMAX produced six stockpiles containing lean ore material from a shaft dug in 1975. The piles were constructed in order to evaluate what drainage problems may occur if Cu-Ni mining were to be developed in Minnesota.

The construction of pile 1 was completed

April 20, 1977. Effluent from the base of the pile was monitored from 1978 to the present by the Minnesota Department of Natural Resources (MNDNR), Division of Minerals. Stockpile samples, effluent and mineralogical data, all from pile 1, were provided by Kim Lapakko, Principal Engineer, Minnesota Department of Natural Resources, Division of Minerals.

Site Description and Geology

Geology of the Babbitt region has been described by Bonnicksen (1972) as being part of the Upper Precambrian Keweenaw formation, comprised of troctolitic gabbro, which consists mainly of calcic plagioclase and olivine. The sulfide minerals in this area generally decrease in concentration from pyrrhotite (Fe_{1-x}S), chalcopyrite (CuFeS_2) to pentlandite [$(\text{Fe},\text{Ni})_9\text{S}_8$]. A grab sample taken from pile 1 was subjected to a mineralogical analysis. The silicate minerals identified from the grab sample, in volume percentages, were; plagioclase (59%), clinopyroxene (11%), olivine (11%), orthopyroxene (3.7%), and amphibole (3.6%). The same grab sample also contained sulfide minerals, in volume percentages, pyrrhotite (0.84%), chalcopyrite-cubanite (0.77%) and pentlandite (0.037%) (Stevenson et al., 1979).

Table 1 contains effluent data from stockpile no. 1 from 10/16/89 to 11/07/91. From the data it is clear that the effluent is continually evolving and has

¹ Paper presented at the 13th Annual National Meeting of the American Society for Surface Mining and Reclamation, May 18-23, Knoxville, Tennessee, 1996.

² Paula D. Kelsey, Masters Degree Candidate, and Ronald W. Klusman, Professor, Dept. Of Chemistry and Geochemistry, Colorado School of Mines, Golden, CO 80401.

³ Kim Lapakko, Principal Engineer, Minnesota Department of Natural Resources, St. Paul, MN 55155.

yet to reach steady state equilibrium with infiltrating meteoric water. Over a period of roughly two years, the pH has dropped from 5.88 to 5.24 (s.u.). Sulfate concentrations have increased almost two-fold, a result highly dependent on fluctuations in transport flow. However, according to Lapakko (1994), the annual sulfate release rate has remained fairly steady, increasing only slightly from 1978-1991, indicating the oxidation of sulfide minerals within the pile. Concentrations of trace metals Co, Cu, Ni and Zn have also increased with time, a result of the decreasing effluent pH over time. Species such as Fe, Mn and Cl were measured in 1981-82 to be roughly 0.02-0.06 mg/L, 0.05-0.13 mg/L and 5 mg/L, respectively. Current data reveals that both Cl and Fe concentrations have remained steady while Mn has increased with time to roughly 5 mg/L. The low content of iron in the effluent indicates that the formation of Fe(OH)₃ within the pile appears to be a possibility, for the appearance of ferric hydroxide under oxidizing conditions occurs at a pH greater than approximately 4.0 (s.u.).

The stockpile is approximately 4 m high and

15 m by 25 m at the base. It was built in four lifts, with lift 1 located at the top of the pile and lift 4 located at the bottom. Samples are identified with three numbers, which represent the pile number, the lift from which it came, and a third number used to distinguish samples from the same lift. An example is 1.3.2, this sample came from pile no. 1, lift 3. Noticeable oxidation was observed in stockpile samples taken from lifts 1 and 2. Visible observations show the samples have a reddish tint to them, while samples taken from lifts 3 and 4 were a medium color gray typical of unoxidized rock. It is hypothesized that the red color was most likely a result of pyrrhotite oxidation, with subsequent precipitation of ferric hydroxide.

Oxidation of Pyrrhotite

Wastes from non-ferrous metal mining operations often contain iron sulfide minerals, made up mostly of mixtures of pyrite (FeS₂) and pyrrhotite (Fe_{1-x}S). Pyrrhotite is particularly important in wastes

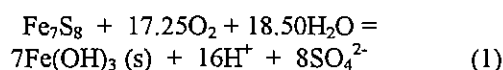
Table 1: Measured effluent concentrations from stockpile no. 1 over a two year period.

Date	pH (s.u.)	SO ₄ (mg/L)	Ca (mg/L)	Mg (mg/L)	Na (mg/L)	Cu (mg/L)	Ni (mg/L)	Co (mg/L)	Zn (mg/L)
10/16/89*	5.88	800	212	54	22	5.90	25	1.90	1.0
11/6/89	5.5	680	166	50	15	5.3	25	2.6	1.0
3/28/90	5.05	290	64	21.4	7.4	10.2	19	10.2	1.01
4/12/90*	5.82	685	148	42	10	9.43	32	1.54	1.54
5/17/90	5.72	1250	286	84	20	10	39	1.91	1.78
6/18/90	5.85	1040	202	70	22	7.78	30	1.27	1.14
7/16/90*	5.79	975	214	66	20	7.82	27	1.25	1.19
8/13/90	5.77	920	228	66	22	5.21	21	1.01	0.93
9/10/90	5.42	940	212	74	18	20	56	2.82	2.27
10/15/90	5.29	1850	358	134	30	35	93	4.35	3.1
11/16/90*	5.31	2400	680	202	54	29	88	4.04	3.55
4/22/91	4.96	1030	194	88	16	19.9	68	2.6	1.8
5/20/91*	5.18	1200	252	107	20	20.3	68	2.4	1.5
6/17/91	5.25	1110	214	104	20	27	71	3	1.6
7/15/91	5.27	1260	278	124	26	21	59	2.4	1.5
8/12/91	5.27	1370	318	110	34	18	54	2.3	1.3
9/9/91*	5.22	1420	268	110	28	30	84	3.4	2.0
10/7/91	5.31	1360	272	108	32	21	67	2.7	1.7
11/7/91*	5.24	1270	252	112	30	27	80	3.2	2.1

* Dates used in geochemical modeling runs.

from mafic rocks. When these minerals are exposed to atmospheric oxygen and water, they are oxidized and release acidity to the environment. Sulfide oxidation, namely that of pyrite, has been thoroughly studied as a major cause of acid mine drainage (Nicholson and Scharer, 1992). Pyrite has received much of the attention because it is found to be prevalent in rocks associated with coal deposits and with most metallic and precious mineral deposits. Although pyrrhotite has not been as extensively researched as pyrite as a contributor of acid generation, in many instances it is the only significant gangue sulfide mineral at the site, as is the case in the Duluth Complex.

The oxidation of pyrrhotite in the presence of water and oxygen is as follows; note that the formula for the monoclinic form of pyrrhotite is Fe_7S_8 , but it is also found in hexagonal forms (Fe_9S_{10}) within the pile (Lapakko and Antonson, 1993). The overall reaction for the oxidation of pyrrhotite is:



where sixteen acidic protons are released for every mole of pyrrhotite oxidized.

Methods

Initial Inverse Geochemical Modeling

The NETPATH modeling program was used to interpret geochemical mass-balance reactions between an initial and final water along a hydrologic flow path (Plummer et al., 1993). The net geochemical mass-balance reaction consists of the masses (per kilogram of water) of plausible minerals and gases which must enter (dissolve) and/or leave (precipitate) the initial water in order to achieve the final water composition. The data base is slightly limited in the number of minerals that it contains, consequently the model was used only to determine the dissolution/precipitation of the more common minerals which contained the major constituents found in the aqueous phases. Also, NETPATH does not include some trace metals which were of interest in this study, such as cobalt, nickel and zinc. This limited the usefulness of the NETPATH program, but it still provided information which made the more complex geochemical modeling easier to manage.

Geochemical modeling of the entire complex system was accomplished using the MINTEQAK (Klusman, 1993) model, which was developed from MINTEQA2 (Allison et al., 1991). The code was modified in order to predict the change in composition

of an aqueous flow as it traverses a wetland/reactor system for treatment of mine drainage. In this application it was used to extend the results of NETPATH by incorporating weathering of solid solutions and weathering of trace constituents.

Sequential Extraction Procedure

The following is a description of the extraction procedure used for 1 g (-270 mesh) of each sample from stockpile no. 1. The sequential extraction procedure used was modified from Tessier and others (1979) and Chao and Zhou (1983). Each sample was placed in a polyethylene centrifuge tube (50 mL) with a lid. After an extraction medium was added, the sample was placed in a sonicator (Bransonic 220). When the allotted time for each extraction had passed, the sample was centrifuged (Damon IEC model K at 14,000 rpm) for 20 minutes. The supernatant was decanted into polyethylene bottles and saved for subsequent analysis. The remaining residue was then rinsed with 10 mL deionized water, centrifuged for 20 minutes and the liquid was decanted and discarded. The next extractant medium in the sequence was then added to the residual sample. This process was used for extractions E1-E4. The extractions were analyzed for metals using a Perkin Elmer Optima 3000 ICP-AES.

Extraction 1 (E1). Water Soluble. The original 1 g samples were leached with 10 mL deionized water for 30 minutes.

Extraction 2 (E2). Exchangeable (Tessier et al., 1979). The residue from E1 was extracted at room temperature for 1 hour with 10 mL of a magnesium chloride solution (1 M MgCl_2 , pH 7).

Extraction 3 (E3). Associated with Iron Oxides (Chao and Zhou, 1983). 20 mL 0.25M $\text{NH}_2\text{OH}\cdot\text{HCl}$ in 0.25 M HCl was added to the residue remaining from E2. This was placed in a 50 °C water bath (P/S Thelco model 84) for 30 minutes with intermittent shaking.

Extraction 4 (E4). Sulfides (Tessier et al., 1979). The residue from E3 was extracted with 3 mL of 0.02 M HNO_3 and 5 mL of 30% H_2O_2 adjusted to pH 2 with HNO_3 and heated in a water bath at 85 °C for 2 hours. A second 3-mL aliquot of 30% H_2O_2 was added and heated again at 85 °C for 3 hours. After cooling, 5 mL of 3.2 M NH_4OAc in 20% (v/v) HNO_3 was added, the sample was then diluted to 20 mL and cooled. The addition of NH_4OAc was to prevent adsorption of extracted metals onto the oxidized sediment (Gupta

and Chen, 1975).

Extraction 5 (E5). Residual (Briggs, 1994). The final residue was digested using a HCl- HNO₃-HClO₄-HF mixture. The samples were quantitatively transferred from the centrifuge tubes to 100 mL Teflon® beakers. To each sample was sequentially added: 15 mL HCl, 10 mL HNO₃, 5 mL HClO₄ and 10 mL HF. All acids were in concentrated form. The samples were then heated to dryness overnight at 110 °C. The next day 5 mL HClO₄ was added to each sample, the temperature was increased to 150 °C and the samples were again heated to dryness overnight. The following day the samples were cooled and to each sample 5 mL aqua regia was added. The samples should be completely dissolved at this point. The solutions were then transferred into 50 mL volumetric flasks and brought to volume with 1% HNO₃. After thorough mixing, the samples were then transferred to polyethylene bottles and saved for later analysis.

Extraction 6 (E6). Total digestion (Briggs, 1994). This extraction was separate from extractions E1-E5. In this case, 0.200 g of fresh sample was totally digested using the same procedure as outlined for E5. Since only one-fifth of the original sample weight from E1-E5 was used, the volume of all acids added was decreased by one-fifth, but the procedure remained the same.

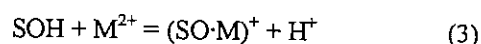
MINTEQAQ Adsorption Modeling

Adsorption of a solute molecule on the surface of a solid can involve removing solvent from the solid surface, then removing the solute molecule from the solution by attaching the solute to the surface of the solid (Stumm and Morgan, 1981). This phenomenon can be described based upon the concept of relative surface excess. For the accumulation of solute *i* at the mineral-water interface, the relative surface excess, Γ_i , or adsorption density of solute *i*, may be defined as:

$$\Gamma_i = n_i / A, \quad (2)$$

where n_i is the moles of surface excess of solute *i* per unit mass of the mineral phase, and A is the specific surface area of the mineral phase. n_i can be defined by two quantities, strong and weak adsorbing surface sites. Strong surface sites refer to a small set of high affinity cation binding sites and the weak surface sites are the total reactive sites available for sorption of protons, cations and anions.

Adsorption of the four trace metals onto ferric hydroxide was achieved using the triple-layer model available in MINTEQAQ. Surface sites are represented as SOH groups where S represents the metals associated with the solid structure, located at the solid-liquid interface. The adsorption of a divalent cation, M^{2+} , onto an adsorption site would be represented by the reaction:



then,

$$K_1 = \frac{[SO \cdot M^+][H^+]}{[SOH][M^{2+}]}, \quad (4)$$

where K_1 is the surface complexation constant.

Results and Discussion

Initial Inverse Geochemical Modeling

Of the twenty possible effluent sampling dates to model, seven dates were chosen in order to model the most varied compositions in the effluent from the pile. It was important to model data at the beginning and end of the sampling time interval as well as during different seasons. Therefore, the first and last effluent sampling dates were chosen to be modeled and the other five dates were selected randomly from the remaining effluent sampling dates. The main objectives of the initial inverse geochemical modeling were:

- 1) Predict what minerals were dissolving and precipitating within the pile and compare predicted minerals to observations from the pile.
- 2) Predict the effluent composition of the pile and compare to measured effluent data.

NETPATH Modeling

Two waters (initial and final) and their actual dissolved concentrations were added into the NETPATH model. The composite rainfall data used as the initial water was obtained from the Marcell Experimental forest in Itasca County approximately 75 miles west of the stockpile (National Atmospheric Deposition Program, 1995). Final water composition was entered into the NETPATH model using effluent data from the pile (Table 1). The Eh of the system was

not measured, but was assumed to be an oxidizing system and entered as 800 mV. Studies conducted to determine the sensitivity of the model to variations in Eh demonstrated that differences in Eh (± 100 mV) did not significantly affect results. Average annual temperature in the area was entered as 3.6 °C. Ripley and Alawi (1986) determined that in the Babbitt region, plagioclase composition was $(Ca_{0.60}, Na_{0.40})Al_{1.36}Si_{2.64}O_8$ and olivine composition was $(Mg_{0.997}, Fe_{1.00}, Ni_{0.003})SiO_4$. These compositions were entered into the geochemical database, so the modeling would reflect actual mineral compositions being weathered. For each specific date, the amount of each mineral within the pile that dissolved/precipitated was recorded in the output of the NETPATH model. The amounts of the minerals for sampling date 10/16/89 that were predicted to dissolve are given in Table 2.

MINTEQAK Modeling

Information obtained through the NETPATH modeling of major mineral constituents was incorporated into the MINTEQAK modeling of the system including all trace metals found in the effluent. All of the models run with MINTEQAK allowed ferrihydrite, montmorillonite, kaolinite, SiO_2 , gypsum, and the hydroxide forms of the four trace metals of interest, Co, Cu, Ni, and Zn to precipitate if supersaturation were to occur. The modeling showed that SiO_2 , montmorillonite and large quantities of ferrihydrite would precipitate, all of which had been verified as precipitates by MNDNR researchers (Table 3). The model did not predict, however the precipitation of gypsum, which had also been identified by MNDNR as a precipitate. It was hypothesized that perhaps gypsum was precipitating with summer evaporation. When evaporation was simulated using MINTEQAK, gypsum did begin precipitation after 15% evaporation.

Table 2: Minerals predicted to dissolve by NETPATH from 10/16/89 effluent data.

Mineral	mg/kg water
Plagioclase	555.1
Olivine	1092.0
Diopside	749.3
Biotite	11.6

The MINTEQAK predicted effluent matched measured effluent very well, with the exception of magnesium (Table 4). The MINTEQAK predicted values for magnesium are high. This suggests that some unknown magnesium mineral may have precipitated in the pile that is not present in the MINTEQAK data base. Available magnesium-containing minerals, such as Mg-nontronite and magnesite, were modeled but none became supersaturated or gave satisfactory results. Downward adjustment of the magnesium content of the olivine being weathered within reasonable limits did not decrease the concentration sufficiently to match the effluent of the pile.

The precipitation of such large quantities of $Fe(OH)_3$ within the pile was considered to be a influential factor which would control the composition of the effluent over time. This led to the hypothesis that trace metals such as cobalt, copper, nickel and zinc were being adsorbed to the large quantities of ferric hydroxide, which was being formed from the oxidation of pyrrhotite and other sulfide minerals. Such a hypothesis would also explain why the trace element hydroxides and carbonates were not predicted to saturate and precipitate by MINTEQAK.

Table 3: Minerals predicted to precipitate by MINTEQAK from 10/16/89 effluent data.

Mineral	mg/kg water
$Fe(OH)_3$	1452.0
SiO_2	696.0
Montmorillonite	714.9

Table 4: MINTEQAK predicted effluent versus actual effluent data for 10/16/89.

Ionic Species	MINTEQAK (mg/L)	Effluent (mg/L)
SO_4^{2-}	801.1	800.0
Ca^{2+}	212.3	212.0
Mg^{2+}	226.0	54.0
Na^+	18.8	22.0
Cu^{2+}	5.91	5.9
Ni^{2+}	23.5	25.0
Co^{2+}	1.89	1.9
Zn^{2+}	0.98	1.0

Iron oxides have long been identified as strong scavengers of trace metals and have been extensively researched in the past (Morgan and Stumm, 1965; Jenne, 1968). They can be present as nodules, concretions, matrix components, cement between particles or as a coating on particles and have been shown to control trace metal distributions in many cases. Hydrous oxide minerals possess proton-bearing surface functional groups and therefore adsorption onto these solid phases is pH dependent. Jenne (1968) determined that sorption by these oxides tend to control Zn and Cu levels in soils. Because of this scavenging ability, it was hypothesized that the iron oxides precipitating in the pile may be adsorbing and perhaps be largely controlling trace metal concentrations such as Cu, Co, Ni and Zn in the effluent.

To verify this hypothesis, the secondary phase ferric hydroxide, and the associated trace metals, were chemically separated from samples within the pile. This was accomplished using the technique of sequential extractions, which allows sediments to be broken down into different mineral associated constituents. After the sequential extractions were performed, concentrations of the trace metals and iron were determined using ICP-AES to see the extent of the adsorption. The E3 extraction would contain ferric hydroxide and associated trace metals, and thus was the extraction of the most interest.

Sequential Extractions

The samples were extracted using the procedure described earlier and were analyzed by ICP-AES. The results discussed below pertain to data from iron and the trace metals of interest: Co, Cu, Ni and Zn with detection limits in ppb: Co (3.42), Cu (0.36), Fe (3.00), Ni (5.79) and Zn (5.33). Extraction E1 (water soluble) held minuscule concentrations of cobalt and nickel and copper, with zinc and iron concentrations less than their detection limits. Extraction E2 was found to have concentrations less than the detection limits for all five metals, indicating that these metals were not weakly adsorbed, but strongly bound to ferric hydroxide. Only the distribution of the metals in extractions E3, E4 and E5 will be discussed, as they are the extractions of primary interest. The results for copper and nickel are plotted in Figures 1-3. It must be noted that although figures for cobalt and zinc are not represented, they similarly follow the same trends as copper and nickel in extractions E3, E4 and E5.

Extraction E3, or the extraction associated with iron oxides, revealed that trace metal

concentrations increase with depth, indicating downward transport by water percolation as the sulfide minerals are weathered. Concentrations of these trace metals were moderate in comparison to the ferric hydroxide concentrations and decreased in the order of $Cu > Ni > Zn > Co$ (Table 5). Iron concentrations in E3 were converted to $Fe(OH)_3$ concentrations and were found to have a relatively constant concentration throughout the pile. Average concentrations for iron and the trace metals are given in Table 5. Extraction E4, associated with sulfides, and the residual extraction, E5 revealed an oxidation pattern for all of the trace metals contained in sulfide minerals, including iron. Weathering of the sulfide (E4) and resistant minerals (E5) were accelerated near the top of the pile and significantly decreased with depth. A notable observation is that an apparent oxidation cut-off is seen at sample number 1.3.2, whereby below this sample in the pile, oxidation is much less. At this depth in the pile it can be concluded that roughly two-thirds of the pile had been oxidized.

Extraction E3, associated with iron oxides, was the extraction of the most interest. Trace metals found in this extraction must have been strongly adsorbed to the ferric hydroxide or they would have been removed by extraction E2, which was designed to remove metal cations which are easily exchanged by other metals, or weakly adsorbed. To verify that strong adsorption had indeed occurred, MINTEQA6 was again employed, this time incorporating adsorption modeling.

MINTEQA6 Adsorption Modeling

Adsorption of the four trace metals onto ferric hydroxide for each of the seven sampling dates originally modeled without adsorption was completed. In order to compare the sequential extraction results from extraction E3 (associated with iron oxides) to the adsorption modeling, it was necessary to determine the type of adsorption occurring onto ferric hydroxide. Weakly adsorbed trace metals would have been stripped from the ferric hydroxide during extraction E2 (exchangeable), leaving only those trace metals which were tightly adsorbed to, or had coprecipitated with the ferric hydroxide in extraction E3. Subsequently, to produce accurate modeling results, site densities (N_s) and surface complexation constants (K_1) for strongly adsorbing species were used in order to simulate as close as possible the conditions under which trace metals would have been originally found in extraction E3 (Dzombak and Morel, 1990).

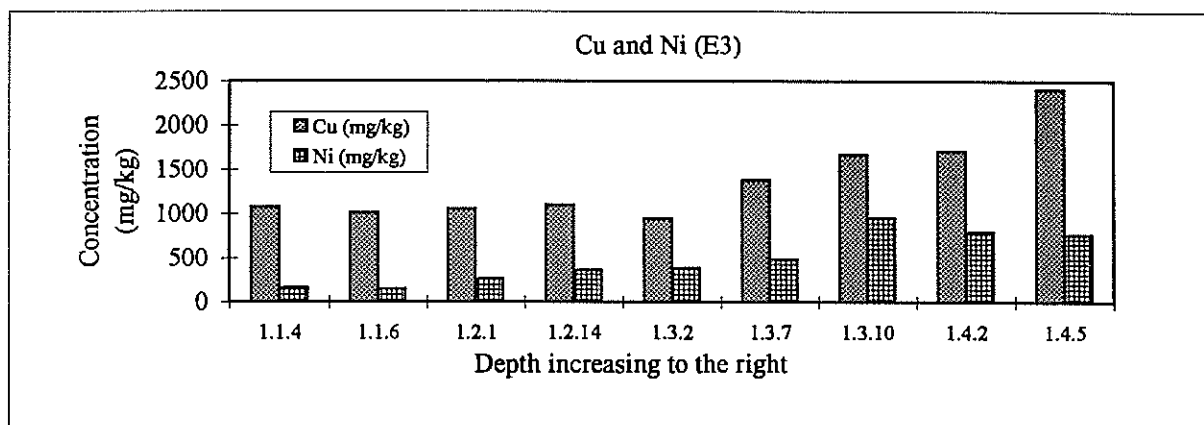


Figure 1. Distribution of copper and nickel concentrations in extraction E3 (associated with iron oxides).

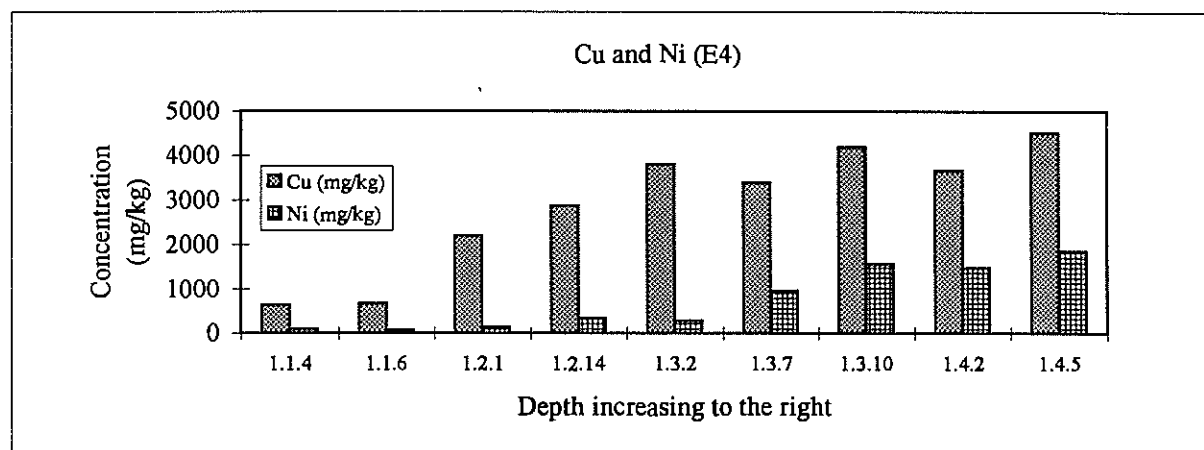


Figure 2. Distribution of copper and nickel concentrations in extraction E4 (sulfides).

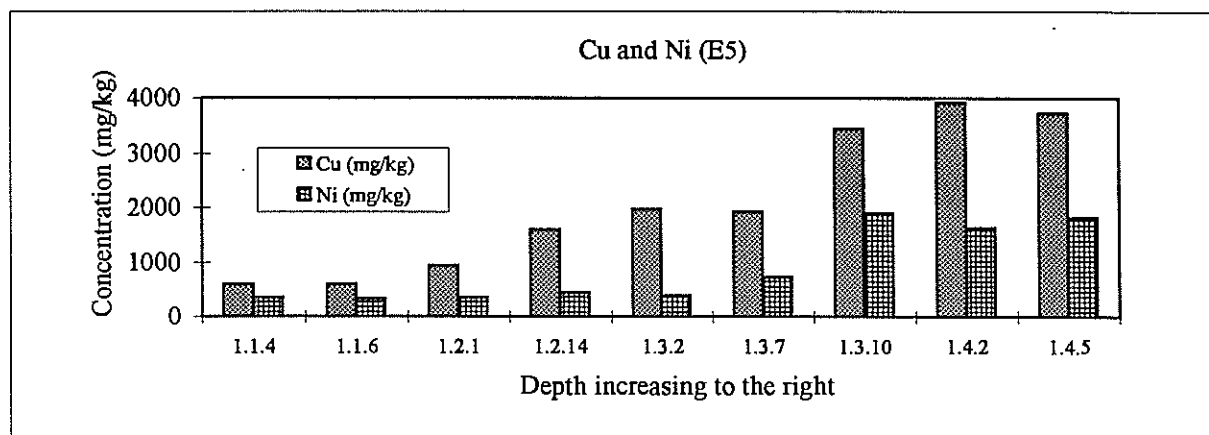


Figure 3. Distribution of copper and nickel concentrations in extraction E5 (residual).

Table 5: Average concentrations (mg/kg) for the elements Co, Cu, Fe, Ni, and Zn in extraction E3.

Element	Average E3 concentration (mg/kg)
Cobalt	18.4
Copper	1740.8
Iron	14680.4
Nickel	460.3
Zinc	64.9

The amount of $\text{Fe}(\text{OH})_3$ available to adsorb trace metals was derived from output data from previous NETPATH trials. The average amount of $\text{Fe}(\text{OH})_3$ precipitated (1.571 g of $\text{Fe}(\text{OH})_3/\text{L}$ of water or 1.5×10^{-2} M) for all seven of the sampling dates modeled was used in order to have a constant amount of $\text{Fe}(\text{OH})_3$. Each of the four trace metals are allowed to compete for sites on the ferric hydroxide surface.

Of the four trace metals, copper was predicted by MINTEQAQ to have by far the highest adsorption. Both nickel and zinc had minor amounts of adsorption onto ferric hydroxide (< 1% adsorption), with nickel adsorption the higher of the two metals. Cobalt was found to have “zero” adsorption onto ferric hydroxide. This result was anticipated since the surface complexation constant for cobalt is negative and because cobalt is present in small concentrations in the effluent. For the elements that were adsorbed, percent adsorption varied depending on the pH of the effluent. Figure 4 suggests that the adsorption of copper decreases with decreasing pH, demonstrating competition with protons in solution. This adsorption relationship with pH is also demonstrated with nickel and zinc, although not as pronounced. Decreasing adsorption can also be attributed to site saturation. As the effluent becomes more acidic, the dissolved concentrations of all four trace metals increase, thus saturating the adsorption sites with both the higher trace metal concentrations and protons, limiting the amount of trace metal adsorption. The ferric hydroxide is no longer capable of adsorbing the increasing concentrations of metals produced by weathering. Other reasons for limitations in adsorption include complexation and competition with other ions in solution, and the high pH_{zpc} of $\text{Fe}(\text{OH})_3$ ($\text{pH}_{\text{zpc}} = 8.0$, Dzombak and Morel, 1990).

The results from the adsorption modeling verify that the trace metals found in extraction E3 were indeed strongly adsorbed to ferric hydroxide. The hypothesis that the strong adsorption sites were

saturated and removed only limited amounts of the trace metals found in the effluent accounts for the small concentrations of trace metals in extraction E3. Both the adsorption modeling, and the measured concentrations of trace metals in extraction E3 confirms that copper was the most strongly adsorbed of the four trace metals, a consequence of high copper concentrations in the effluent and its strong complexation constant. Zinc concentrations in E3 and predicted adsorption onto ferric hydroxide had good correlation. Adsorption of cobalt was predicted by the modeling to be nonexistent, but minute amounts of Co in extraction E3 suggests that slight adsorption was taking place. Modeling and sequential extraction results, however differed in amounts of nickel and zinc adsorbed in extraction E3 and predicted to adsorb by MINTEQAQ. The modeling predicted that nickel had adsorbed much less than copper, and in similar amounts as zinc, but the sequential extraction results demonstrated that adsorbed nickel concentrations were much closer in concentration to copper than zinc.

This inconsistency can be attributed to the inability of the model to accurately predict the influence of elements in high concentration in solution on adsorption. The high concentrations in the effluent increased adsorption, an influence poorly modeled.

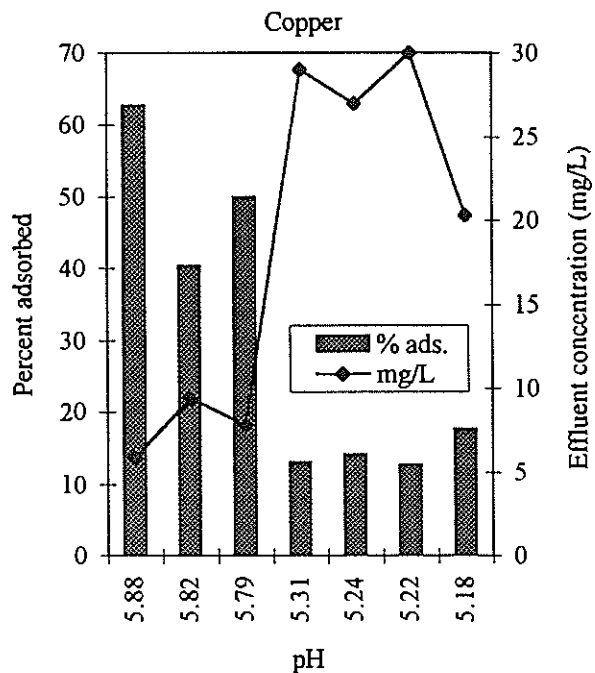


Figure 4. Percent adsorption of copper using MINTEQAQ and concentration of copper in the effluent as a function of pH for seven sampling dates.

The fact that nickel adsorbed more than was predicted may verify research by Benjamin and Leckie (1981), who hypothesized that many of the strong binding sites for one metal are not preferred binding sites for other metals. This implies that nickel may have specific sites to which it is attracted to, which then inhibits adsorption by other metals with higher complexation constants. This site selectivity would not be compensated for in the model using simple surface complexation constants.

Summary and Conclusions

The primary objective of this research was to determine the nature of the weathering processes which were occurring within the pile and the effects of these processes on water quality. The evidence presented here illustrates that geochemical modeling was effectively used to confirm observations of minerals that were dissolving/ precipitating within the pile. Geochemical modeling was also effective in supporting evidence of the adsorption of trace metals onto ferric hydroxide found in the extraction E3, or associated with iron oxides. Because adsorption of trace metals onto ferric hydroxide is minor, precautionary measures should be taken if Cu-Ni mining in the Duluth Complex develops. Rates of oxidation and weathering of sulfide minerals should be slowed as much as possible. This can possibly be achieved by the use of a layering system, consisting of polyethylene liners, soil and vegetation, covering the pile. Alternately, reduction of meteoric water input will also slow oxidation. This will help in the retardation of the oxidation and weathering processes, which result in the release of toxic levels of trace metals in the effluent and possibly to ground water as well.

Literature Cited

Allison, J.D., Brown, D.S., and Novo-Gradac, K.J. 1991. MINTEQA2/PRODEFA2, A Geochemical Assessment Model for Environmental Systems: Version 3.0 User's Manual, U.S. EPA, #EPA/600/3-91/021, 106 p.

Benjamin, M.M. and Leckie, J.O. 1981. Competitive adsorption of Cd, Cu, Zn and Pb on amorphous iron hydroxide. *J. Colloid Interface Sci.* 83: 410-419.

Bonnichsen, B. 1972. Sulfide minerals in the Duluth Complex. p. 388-393. *In: Geology of Minnesota: A Centennial Volume.* (P.K. Sims and G.B. Morey, Eds.) Minnesota Geological Survey.

Boucher, M.L. 1975. Copper-nickel mineralization in a drillcore from the Duluth Complex of northern Minnesota. U.S. Bureau of Mines IC 8084, 55 p.

Briggs, P. 1994. U.S.G.S., Denver, CO. Personal communication.

Chao, T.T., and Zhou, L. 1983. Extraction techniques for selective dissolution of amorphous iron oxides from soils and sediments. *Soil Society of America Journal.* 47: 225-232.
<https://doi.org/10.2136/sssaj1983.03615995004700020010x>

Dzombak, D.A., and Morel, F.M.M. 1990. *Surface Complexation Modeling: Hydrous Ferric Oxide.* John Wiley and Sons, Inc. USA, 393 p.

Gupta, S.K. and Chen, K.Y. 1975. *Environmental Letters.* 10: 129-158.
<https://doi.org/10.1080/00139307509435816>

Jenne, E.A. 1968. Trace Inorganics in Water. p. 337-387. *In: Advances in Chemistry Series 73.* (R.A. Baker Ed.).

Johnson, R.G. 1970. Economic geology of a portion of the basal Duluth Complex, Northeastern Minnesota. Ph.D. Thesis, Univ. Iowa, Iowa City, Iowa. Dissertation Abs. No. 70-23907, 180.

Klusman, R.W. 1993. Computer Code to Model Constructed Wetlands for Aid in Engineering Design: Application of a Computer Code to the Modeling of Biogeochemical Processes Operating in Constructed Wetlands and Anaerobic Reactors. Report, #JO219003, March 1993, Bureau of Mines, U.S. Department of the Interior, vol I, 11.

Lapakko, K.A. and Antonson, D.A. 1993. Oxidation of sulfide minerals present in Duluth Complex rock: A laboratory study. p. 593-607. *In: Environmental geochemistry of sulfide oxidation.* ACS Symposium Series No. 550 (C.N. Alpers and D.W. Blowes, eds.), American Chemical Society, Washington, D.C.

[https://doi.org/10.1016/0021-9797\(81\)90337-4](https://doi.org/10.1016/0021-9797(81)90337-4)

- Lapakko, K.A. 1994. Comparison of Duluth Complex rock dissolution in the laboratory and field. p. 419-428. *In*: International Land Reclamation and Mine Drainage Conference and Third International Conference on the Abatement of Acidic Drainage, vol I. Bureau of Mines, SO 06A-94.
<https://doi.org/10.21000/JASMR94010419>
- Morgan, J.J. and Stumm, W. 1965. International Water Pollution Res. Conference Proc., 2nd, Tokyo. pp. 103.
- National Atmospheric Deposition Program. 1995. Natural Resource Ecology Laboratory. Colorado State University. Fort Collins, CO 80523. (303) 491-1975.
- Nicholson, R.V. and Scharer, J.M. 1992. Laboratory studies of pyrrhotite oxidation kinetics. p. 15-25. *In*: Environmental geochemistry of sulfide oxidation. ACS Symposium Series No. 550 (C.N. Alpers and D.W. Blowes, eds.), American Chemical Society, Washington, D.C.,
- Plummer, L.N., Prestemon, E.C and Parkhurst, D.L. 1993. An Interactive Code (NETPATH) for Modeling Net Geochemical Reactions Along a Flow Path. Water-resources Investigations Report 91-4078, U.S. Geological Survey, revision 1.3 BETA, 227 p.
- Ripley, E.M. and Alawi, J.A. 1986. Sulfide mineralogy and chemical evolution of the Babbitt Cu-Ni deposit, Duluth Complex, Minnesota. *Canadian Mineralogist* 24: 347-368.
- Sims, P.K. 1967. Exploration for copper-nickel in Northeastern Minnesota. *Skillsings Mining Review* 56 (8): 6-7.
- Stevenson, R.J., Kreisman, P.J. and Sather, N.P. 1979. Minnesota regional Cu-Ni study, Vol. 3, Chap I. Minnesota Environmental Quality Board, 70 p.
- Stumm, W. and Morgan, J.J. 1996. *Aquatic Chemistry*, 3rd Ed. John Wiley & Sons, Inc. USA, 1022 p.
- Tessier, A., Campbell, P.G.C. and Bisson, M. 1979. Sequential extraction procedure for the speciation of particulate trace metals. *Analytical Chemistry* .51: 844-851.
<https://doi.org/10.1021/ac50043a017>